Nuclear Inst. and Methods in Physics Research, A 928 (2019) 58–64

Contents lists available at ScienceDirect

Nuclear Inst. and Methods in Physics Research, A

journal homepage: www.elsevier.com/locate/nima

Compensation of longitudinal entrance and exit gap field effects in RFQ's of the 4-ROD type

M. Schuett *, M. Syha, U. Ratzinger

Institute of Applied Physics, Goethe-University, Frankfurt am Main, Germany

ARTICLE INFO

Keywords:
4-ROD RFQ
RFQ
Fringe field
Ladder-RFQ
Gap field

ABSTRACT

In case of 4-Rod-type RFQ's the quadrupole electrodes are excited by a series of coupled RF oscillators. As the contact planes between both electrode pairs differ, there remains an oscillating electric potential along the beam axis. This results in remarkably high longitudinal field components between the electrode ends and the RFQ tank end walls. In contrast, the electrodes of a 4-Vane RFQ are equally charged to $\pm|V_0/2|$ and only feature a quadrupole on-axis field. The entrance gap fields were investigated to serve as a longitudinal prebuncher instead of causing additional longitudinal emittance growth. The effects of the entrance gap field have been validated in beam dynamics simulations. The exit fields have to be taken into consideration for a calculation of the exact RFQ output energy.

1. Introduction

Two classes of RFQ resonators are used. One is the 4-Vane RFQ cavity, which applies the $H_{21(0)}$-mode. If properly tuned the quadrupole shows perfect symmetry, the electrode pairs oscillating at voltage amplitude $\pm V_0/2$, V_0 being the vane–vane-amplitude. The major challenges in that case are a proper RF design and a tuning concept to get rid of the $H_{11(0)}$ dipole modes, which can occur at an identical resonance frequency as the quadrupole mode.

Alternatively, the 4-Rod-type RFQ's are used, traditionally at the lower frequency range. They are compact and cost efficient. In this case, challenges are given by water cooling techniques and by the presence of a non-zero on axis potential along the beam axis due to the excitation of the quadrupole electrodes by a certain number of coupled oscillators along the beam axis. A main consequence of that concept on the beam is a remarkable longitudinal electric field component along the entrance and exit gaps between electrodes and tankwalls. Ref. [1] describes the measured exit energy shift by the RFQ end gap in detail for one case.

At the beginning of the RFQ electrodes a radial matcher accepts the incoming dc beam reducing the aperture to the mean aperture before the beam is prepared for the bunching process. The length of the radial matcher is usually fixed to an integer multiple of $\beta\lambda$. In contrast, the high energy end of the electrodes is continuously adjustable in both length and phase. The first solution for ending cells of electrodes was proposed by Crandall [2]. By calculating the electric exit field the ending electrode shape could be adjusted according to the equipotential lines of a certain radial matching potential function satisfying Laplace's equation. The method had two drawbacks. First, adjacent electrodes differed in length and second, the transition to the field free region outside the RFQ was not smooth at all. Another approach was made by Iwashita and Fujisawa in 1992 [3] by introducing half cells. The electrodes should end near to the quadrupole symmetry position in the middle of an RFQ unit cell, where the aperture is r_0. The nowadays applied standard solution was again proposed by Crandall in 1994 [4]. He established a transition cell at the end of the electrodes. Instead of terminating the electrodes at mid-cell aperture a smooth transition is performed from full to zero modulation. The on-axis field at the end of the transition cell, given by a three-term potential, becomes zero. The transition cell can be seen as a quadrupole focusing transport channel. By adjusting its length of zero modulation at the high energy end of the electrodes the Twiss parameters of the beam ellipse in both transversal planes can be matched and the exit phase of the particles can be determined. Accordingly, the influence of the exit gap field can be reduced to a minimum. The energy shift along the exit gap field will be minimized if the synchronous particle had a phase of $\varphi_0 = \pm 90°$ at the effective gap center between the electrode ends and the tank wall of the RFQ.

So far, the longitudinal gap field in the entrance gap between the entrance flange and the radial matcher in 4-ROD type RFQs has been neglected. In this paper, we introduce a strategy to use the entrance gap field as a single prebuncher cell by adjusting the radial matcher length manually (s. also [5]). Furthermore, the electrode connections to the resonator have to be taken into consideration with respect to the field orientation (cf. Fig. 4).

* Correspondence to: IAP, Goethe-University Frankfurt, Max-von-Laue-Straße 1, 60438 Frankfurt am Main, Germany.
E-mail address: schuett@iap.uni-frankfurt.de (M. Schuett).
URL: http://beschleunigerphysik.uni-frankfurt.de/ (M. Schuett).

https://doi.org/10.1016/j.nima.2019.02.071
Received 9 November 2018; Received in revised form 27 February 2019; Accepted 27 February 2019
Available online 7 March 2019

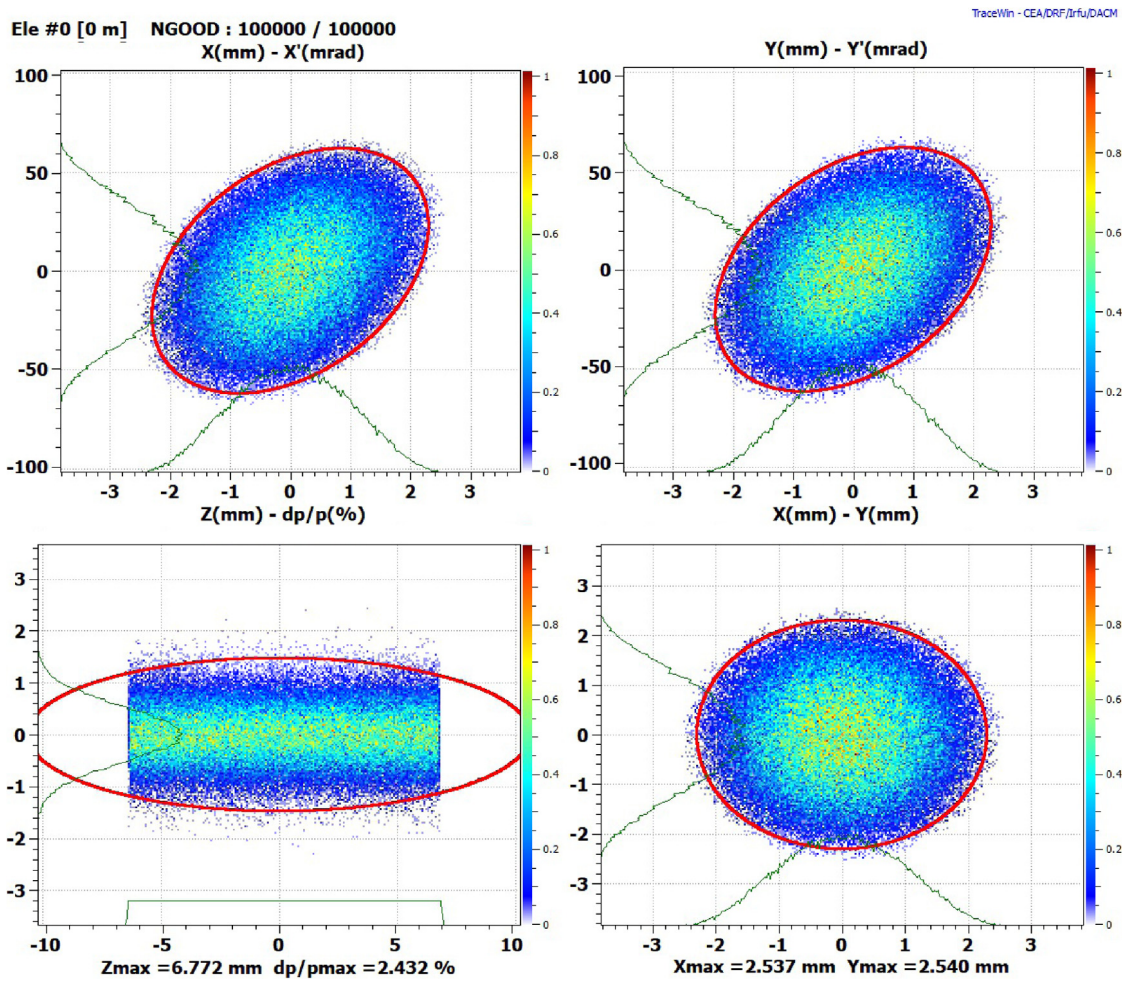

Fig. 1. Phase space plots at the beginning of the electrodes (at the radial matcher) including the 99%-ellipses (red, color in online version) for backward simulation to the entrance flange. The input parameters at the electrodes serve as a basis for the beam dynamics simulation with PARMTEQM (RFQGen) [6].

2. Entrance gap field

To reduce any RF radiation losses throughout the beam entrance and exit flanges, their apertures should be kept as small as possible. Yet, the aperture should be considerably larger than the maximum beam envelope. The parameters used for the calculations presented in this paper are subject to the specifications and beam dynamics calculations [7,8] of the Ladder-RFQ [9,10] for the FAIR p-Linac [11]. The main parameters of the Ladder-RFQ are shown in Table 1. As the RFQ beam dynamic calculations start between the tank wall and the beginning of the electrodes, the beam envelope is simulated backwards towards the Low Energy Beam Transfer line (LEBT) including space charge effects. As a typical example for high current proton RFQ's the input emittance of the RFQ beam dynamics simulation with $\varepsilon_{rms,norm} = 0.3\ \pi$ mm mrad is a 4D waterbag distribution with Twiss parameters $\alpha = 0.7$ and $\beta = 0.04$ mm/mrad (also known as Courant–Snyder parameters).

The parameters of the beam with a negative α serve instead as the input beam parameters to simulate the beam envelopes backwards to the entrance flange (s. Fig. 1). The beam transport in this drift section was calculated with TraceWin.[1] For an aperture shaped entrance flange with a diameter increase from 18 mm to 28 mm towards the inner side of the cavity (s. Fig. 2), the 100% envelope remains well below the aperture.

[1] For more information cf. http://irfu.cea.fr/.

Table 1
Main parameters of the ladder-RFQ.

Frequency	325.224 MHz
Electrode length	3330 mm
Number of RF cells	55
Number of RFQ cells	245
Vane-vane-voltage	88.4 kV
Design current	100 mA
W_{in}	95 keV
W_{out}	3 MeV
$(\beta\lambda)_{in}$	13.12 mm
$(\beta\lambda)_{out}$	73.54 mm

Besides an appropriate transverse beam matching, the beam is exposed to longitudinal gap fields at the entrance gap. Due to the different mounting points of both electrode pairs, the "RF potential" oscillates along the beam axis (s. Fig. 4). As a consequence, the longitudinal on axis field integral between the grounded entrance flange and the electrode entrance plane (s. Fig. 3) is not zero. These peaks in the longitudinal on-axis field distribution at both the entrance and exit of the RF electrodes have not been considered so far in beam dynamics calculations and codes. Therefore, an energy modulation is imposed on the beam after passing that gap field and arriving at the entrance plane of the electrodes, which may be disadvantageous for the beam dynamics of the RFQ low-energy end, depending on the relative RF phase. In contrast, the electrodes of 4-Vane RFQ's have a symmetric potential $\pm V_0$ and do not generate an overall longitudinal gap field. Longitudinal gap fields occur in all 4-ROD type RFQ's, e.g. classical

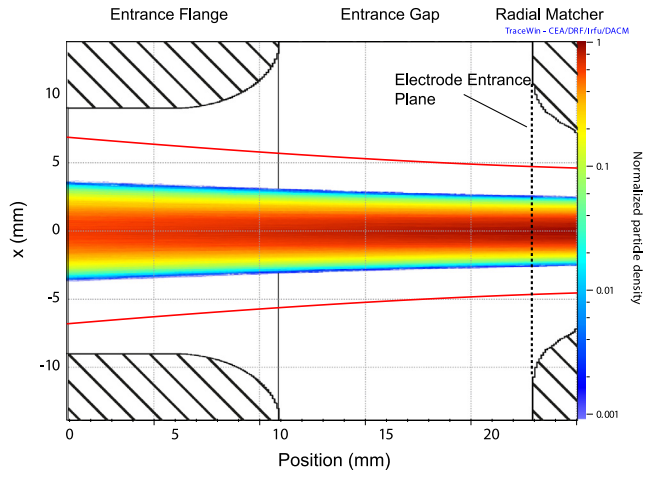

Fig. 2. Result of the beam dynamics simulation at the RFQ entrance. The density plot illustrates the normalized particle density along the drift between the entrance flange and the radial matcher. A total drift of 25 mm and an aperture of 18 mm at the entrance flange are adequate to avoid any particle losses. The 100% beam envelope is plotted in red (color in online version).

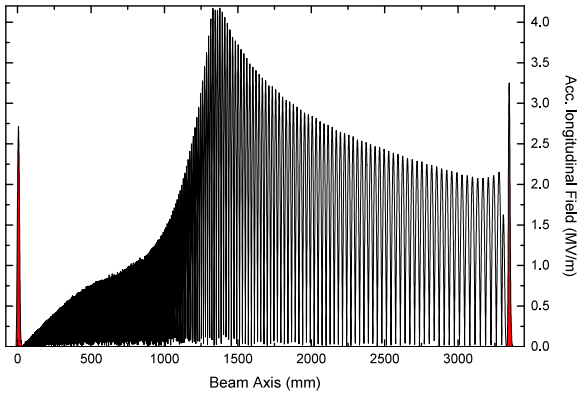

Fig. 3. Longitudinal electric field distribution along the beam axis of the RFQ. The field of the entrance gap and of the exit gap (first and last peak, respectively) are significantly larger compared to the field of single RFQ cells, especially at the beginning of the modulation. The data are the results of a 3D electrodynamical simulation involving the entire modulation of the electrodes. The simulations were evaluated with CST microwave studio.

4-ROD, Ladder-, Spiral-, IH- or Split-Coaxial RFQ's. The net on axis E-field resulting from the gap field increases for a smaller beam flange diameter, which was designed to be as small as possible in the previous step, in order to avoid RF radiation losses. Yet, rounding the inner edges of the entrance flange resembling the radial matcher entails two major advantages: First, the entrance field is more symmetrical as the radial shape of the flange geometry is similar to the radial matcher simplifying a determination of an effective gap center. And second, the rod-wall capacity is reduced, which results in a reduction of the gap voltage (s. Fig. 6) and of the gap field.

On the low energy side of the RFQ, a dc beam is entering. Consequently, the entrance phase range covers 2π. Still, the influence of the gap field can be suppressed by the following strategy. First of all, the integral of the longitudinal electric gap field is minimized by an optimization of the distance between tank wall and first modulated RFQ cell, which follows directly behind the radial matcher. Actually, the entrance gap (s. Fig. 2) is varied to reduce the gross acceleration voltage caused by the longitudinal gap field. The longitudinal electric field distribution along the beam axis is plotted in Fig. 5. The integral of the gap field $\int E_z(r = 0)\, dz$ from $z = 0$ to $z = L_g$ is shown in Fig. 6 in dependence of the entrance gap length d. A gap

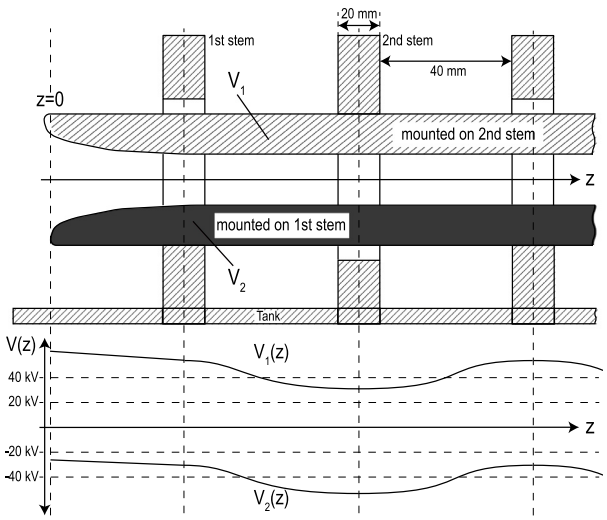

Fig. 4. Electrode "potential" of the 4-ROD-type ladder-RFQ along the beamline estimated from CST simulations. The vane–vane voltage is given by $V_2 - V_1$, remaining constant along z. The on axis potential between the electrodes at $z = 0$ is given by $V(z = 0) \approx (V_2(0) + V_1(0))/2$.

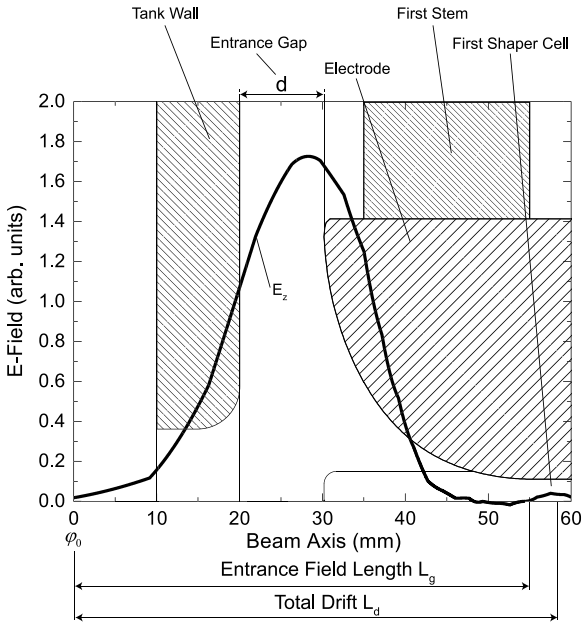

Fig. 5. Course of the gap field (longitudinal electric field component E_z along the beam-axis) from the entrance flange into the tank to the beginning of the first shaper cell of the electrodes at $z \approx 55$ mm.

length d above 20 mm does not further reduce the voltage by more than approx. 5%. Nevertheless, the final distance cannot be chosen ad libitum. For a successful beam matching between LEBT and RFQ the preceding focusing optics (e.g. a solenoid) in front of the RFQ has to be capable of focusing the beam into the radial matcher. Regarding an emittance growth by space charge effects, the drift for the space-charge decompensated beam within the cavity has to be as short as possible. The maximum length is therefore limited. In case of the Ladder-RFQ, a gap length d of around 15 mm seems to be a reasonable compromise between a reduced gap field and a tolerable space charge action. For smaller distances the gap field would increase and, otherwise, the beam matching was barely reachable for a larger distance at a design beam current of 100 mA.

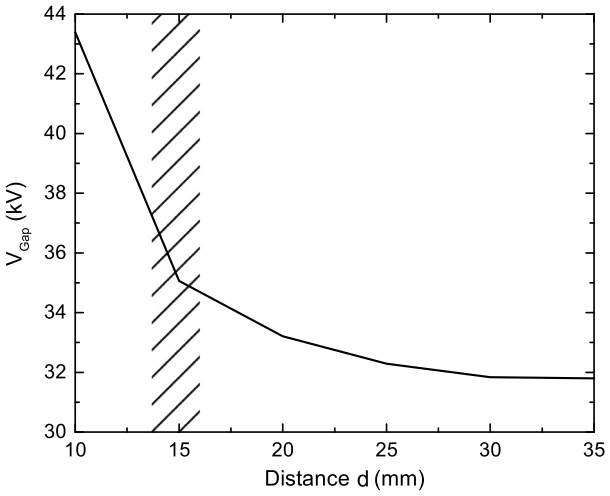

Fig. 6. Potential amplitude from the entrance flange to the center of the first cell along the beam-axis in dependence of the gap distance d as defined in Fig. 5. The suitable range for a reasonable compromise between a reduced gap field and a tolerable space charge action is shaded.

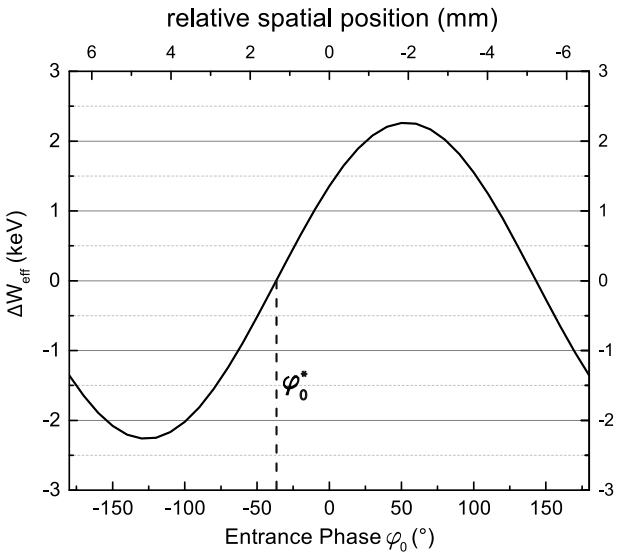

Fig. 7. Energy gain along the gap field in dependence of the entrance phase φ_0 and particle position, respectively. The energy gain is zero at φ_0^*.

3. Phase matching and electrode length adjustment

The next challenge is to calculate the effective net energy gain ΔW_{eff} along the entrance field, which has a length of approx. nine times $\beta\lambda/2$ for 325 MHz at 95 keV. The total net energy gain ΔW_{eff} is obtained by integration of the longitudinal electric field along the path L_g of the entrance gap regarding the RF entrance phase φ_0. Since the electric field of the gap is not completely symmetrical, it is not possible to find an analytical expression for the energy gain. The numerical integration of the field across the entrance gap at positions $z_i = i \cdot \delta z_i$ is given by:

$$\Delta W_{eff}(\varphi_0) = \int_0^{L_g} E_z(z,t)\cdot dz = \sum_i E_{z,0}(z_i)\cdot \delta z_i \cdot \cos\left(\varphi(z_i)+\varphi_0\right) \quad (1)$$

with $\varphi(z_i) = 0$ for $i = 0$. For the Ladder-RFQ example, the energy gain is plotted in Fig. 7 as a function of the incoming phase φ_0. The incoming phase width of a "dc beam bunch" is 360°, which refers to a spatial width of $\beta\lambda \approx 13.1$ mm. Fig. 7 shows the energy modulation of that beam segment with a length of $\beta\lambda$ after passing the gap. If the distance between entering the longitudinal entrance gap field and the mid of the first RFQ shaper cell is L_d, the passed phase shift for that drift is approximately (when neglecting the energy variation):

$$\Delta\varphi(L_d) \simeq \omega \cdot \frac{L_d}{\beta c} \quad (2)$$

The energy gain at the rising edge becomes zero for $\varphi_0 = \varphi_0^*$, resulting in:

$$\Delta W_{eff}(\varphi_0) = W_0 \cdot \cos(\varphi_0 - \varphi_0^* - \pi/2) \quad (3)$$

By RFQ design, the synchronous phase at the mid plane of the first shaper cell is −90°. The prebunching effect of the gap field will be profitably used, if the particles passing the gap field without an energy gain on the rising edge of the energy modulation at φ_0^* arrive at the center of the first cell with a phase of $\varphi_0 = -90°$. To fulfill that condition the total drift L_d has to be adjusted by an additional drift L_{cor} in order to get:

$$\varphi_0^* + \Delta\varphi(L_d + L_{cor}) = -90° \pm n \cdot 360° \quad (4)$$

Eq. (4) is valid for the geometry as plotted in Fig. 8. In that case, the gap field is in parallel with the field in the first shaper cell. However, if the stem connections are exchanged between rod pairs, or if the modulation starts in opposite direction at the first shaper cell, Eq. (5) has to be used instead of Eq. (4):

$$\varphi_0^* + \Delta\varphi(L_d + L_{cor}) = +90° \pm n \cdot 360° \quad (5)$$

For example, in case of the Ladder-RFQ for the p-Linac Eq. (5) is valid. With the parameter for the total drift of $L_d = 57.9$ mm, an entrance phase $\varphi_0^* = -37°$ (cf. Fig. 7) and $n = 4$ one gets from Eq. (5):

$$\Delta\varphi(L_d + L_{cor}) = +90° + 37° + 4 \cdot 360° \quad (6)$$

and therefore for the total drift:

$$L_d + L_{cor} = \frac{1567°}{360°} \cdot 13.1 \text{ mm} \quad (7)$$

with

$$L_{cor} = -0.9 \text{ mm}. \quad (8)$$

The total drift length will have to be shortened between the entrance and the first RFQ shaper cell by L_{cor} in order to attain the appropriate phase and to comply with Eq. (5). Therefore, either the gap length can be adjusted directly by matching the inner tank length, if the electrode geometry ought not to be changed, or, alternatively, by modifying the electrodes itself. As a consequence the entrance phase will also be changed and has to be reviewed in an iterative process (cf. Fig. 9).

The electrode length adjustment has to be realized within the radial matching section. For small values of L_{cor} (< 2 mm) the radial matching section could be shortened by a steeper decrease of the aperture. As a third solution the electrodes only could be shifted longitudinally against the cavity mid plane.

Alternatively, if the entrance drift reduction results in mechanically impractical values, the electrodes could be extended within the radial matching section by applying Eq. (4) and designing the mounting of the electrode pairs appropriately. For the Ladder-RFQ, that would result in a length correction of $L_{cor} = 5.7$ mm. At the end of the radial matcher an additional quadrupole focusing channel with constant mean aperture r_0 and a length of L_{cor} has to be inserted in such a case. For the Ladder-RFQ example, the strategy by shortening the electrodes according to Eq. (8) is clearly preferable.

An adjustment of L_{cor} by a change of the gap lengths, both at the entrance and exit, will then modify the effective lengths of the gap fields, appropriately. As a consequence, the zero crossing entrance phase φ_0^* will also have to be recalculated (s. Fig. 7). In case of the

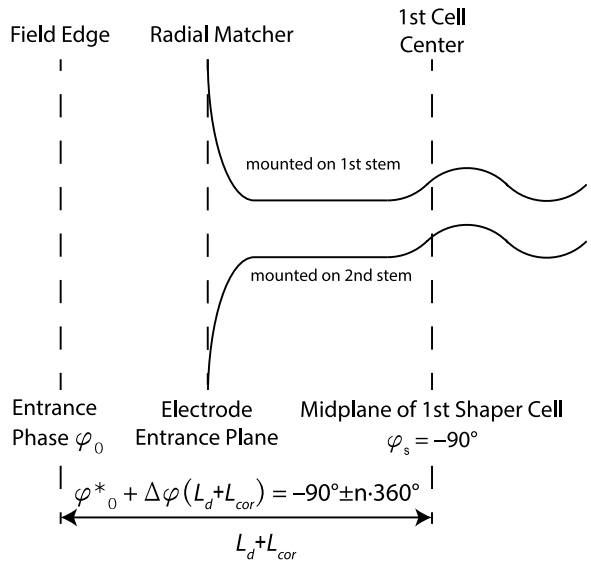

Fig. 8. Schematic illustration of the phase difference between the entrance gap field edge and the first cell midplane. The outlined electrodes each represent a vertical and a horizontal electrode pair. The upper one is mounted to the first stem and the lower one is mounted to the second stem, respectively. For a better visualization the modulation and distances are not to scale.

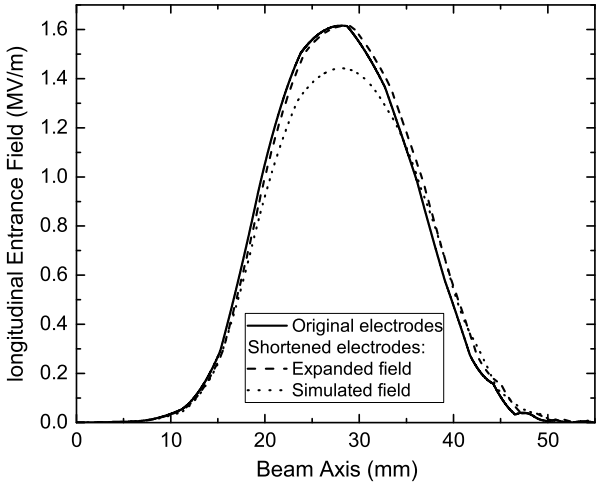

Fig. 9. On-axis gap fields for the ladder-RFQ. The black curve applies for the original gap geometry. The dashed curve shows the same curve stretched by 2.5 mm. The dotted curve represents the result from a 3D electrodynamical field simulation.

Ladder-RFQ, that effect on φ_0^* could be predicted by expanding the original field (s. Fig. 9). Both the stretched and simulated curve for an extended gap result in about the same φ_0^* (cf. Fig. 7). Only the energy variation amplitude is reduced by the real field. That knowledge of a stable φ_0^* allows an iterative determination of the final length correction without having to simulate every single length deviation.

The impacts on the beam dynamics of an energy modulated beam in respect to the phase has been validated by the transport through the RFQ. Therefore, two input distributions have been used. One represents the optimized case, when the rising edge of the energy modulation arrives at a synchronous phase of $\varphi_0 = -90°$ at the center of the first RFQ cell after the radial matcher. The other one is shifted by 180° arriving at $\varphi_0 = +90°$ which constitutes the "worst" case. The total nominal input energy of 95 keV is modulated by ±3.8 keV at a beam current of 100 mA. Both entrance phase space distributions are shown in Fig. 10 and the results of the beam transport through the Ladder-RFQ calculated by PARMTEQM (RFQGen) are summarized in

Table 2
Results of the beam dynamics simulations at the RFQ exit. The normalized rms input emittance is 0.3 π mm mrad.

Beam parameter	Optimized case $\varphi_0 = -90°$	Reference case w/o gap field	Mismatched case $\varphi_0 = +90°$
Transmission	87%	86%	73%
$\epsilon_{x,n,rms}$ (π mm mrad)	0.31	0.33	0.34
$\epsilon_{y,n,rms}$ (π mm mrad)	0.31	0.32	0.34
$\epsilon_{z,n,rms}$ (π deg MeV)	0.20	0.21	0.27
Transversal emittance growth	3%	10%	13%

Table 2. Additionally, both cases have been compared with a reference cw beam without a gap field, which is therefore not energy modulated. The transmission increases, and emittances are reduced for the case of a matched phase, which is a result of an advantageous pre-bunching effect of the entrance gap. On the contrary, both transmission and emittances are deteriorated, if the phase of the energy modulated beam was completely mismatched to the RFQ. The negative impact on the beam dynamics will be considerably increased, if the modulation exceeded 5% of the nominal input energy. For an energy modulation above that threshold also the matched phase does not improve beam parameters any longer. Yet, an universal valid outcome cannot be specified and the effect of the entrance gap ought to be investigated individually for every single case.

4. Effects of the exit gap field

In comparison to the cell length ($l = \beta\lambda/2 = 36.8$ mm in our example for a nominal output energy of 3 MeV [8]) at the high energy end, the exit gap is rather short. For the Ladder-RFQ, the ratio between the gap length and the exit cell length is approx. 0.3. The transient time factor accordingly is around 0.9 and the energy gain is determined by the synchronous RF phase at the mid-plane of the exit gap. The maximum effect on the beam energy of our example results in up to ±30 keV. The synchronous phase at the center of the last accelerating cell in case of the Ladder-RFQ is $\varphi_0 = -22.4°$. At the exit gap mid-plane the synchronous phase then becomes $\varphi_0 = -39.9°$, or $\varphi_0 = +140.1°$, resulting in an energy gain of ±23 keV: The sign depends on the mounting of the electrodes as the potential of the gap field is defined and caused by that pair of electrodes which are connected second to the last stem, respectively.

For a proper beam matching to the following DTL structures the RFQ design energy has to be met. In case of a resulting energy mismatch, in most cases an energy slightly above design energy is preferable: Reducing the entrance gap voltage of the following DTL is "safer". In case of "KONUS" beam dynamics an injection energy above "nominal" is easily corrected by an adequate phase setting of the DTL, while lower injection energies may cause emittance growth [12]. In order to gain an acceleration of the bunch within the last accelerating cell of the accelerating section (s. Fig. 11), the electric field has to be appropriately oriented. I.e. the potential of the "upper" electrode pair has to have a negative potential and the other pair a positive potential while the bunch is approaching that cell. As the mid gap distance between the last accelerating cell and the exit gap is approx. $3 \cdot \beta\lambda/2$ the "upper" pair is positively and the "lower" pair negatively charged as the bunch passes the exit gap. Consequently, the "lower" electrode pair has to be fixed at the last stem, so that the "upper" pair determines the evolution of the potential within the exit gap leading to an additional acceleration of the bunch within the exit gap field. Meeting the specified RFQ exit energy exactly means then to just include the effect of the exit gap in the simulations.

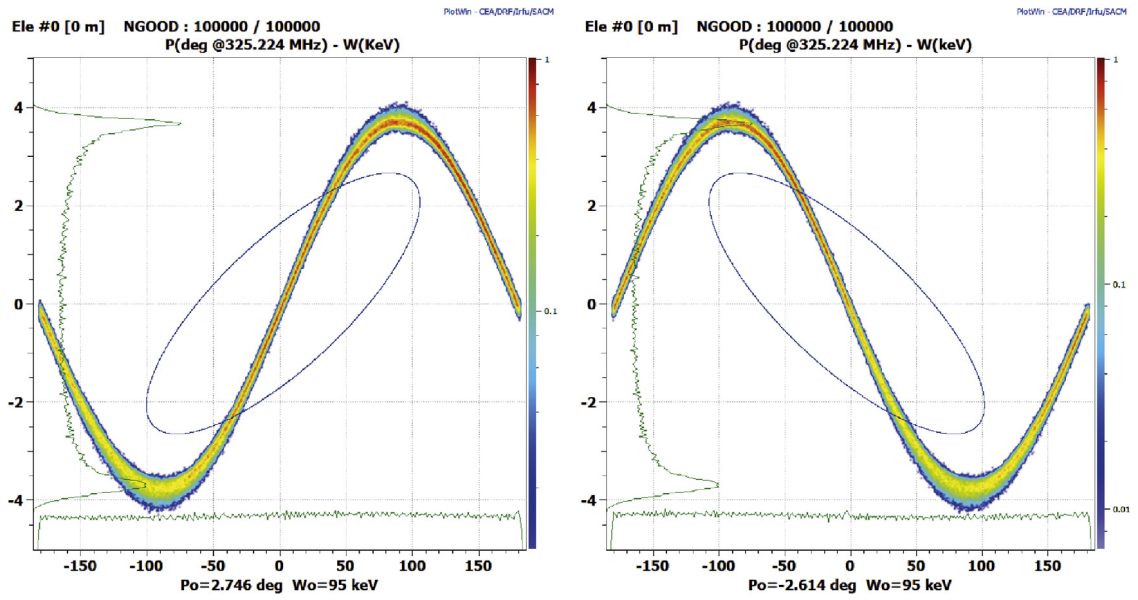

Fig. 10. Input distributions of the energy vs. phase for the transport simulations through the RFQ. The left case refers to an optimized case, where the rising edge of the energy modulation passes the center of the first modulated RFQ cell at $\varphi_0 = -90°$ and the right one to a fully mismatched ("worst") case at $\varphi_0 = +90°$ (color in online version).

5. Conclusions

This work presents a possibility to advantageously utilize the entrance gap in 4-Rod like RFQ structures for prebunching. As a consequence, the bunching effect of the RFQ is supported and the effect of the longitudinal gap field cannot act against the bunching process within the shaper section. By supporting the bunching effect even before particles enter the RFQ electrodes one can expect to either reduce particle losses within the buncher section or to cut down the length of the bunching section of the RFQ to have a shorter structure. Summarizing, the general guide for reducing gap field effects for 4-Rod RFQ's at the entrance and exit reads:

- Optimization of the tank-to-electrode distance by analyzing the longitudinal 3D fields, which is a tradeoff between the absolute gap voltages and maximum tolerable drift lengths.
- Calculating the energy gain in dependence of the entrance phase for the drift to the first shaper cell. In order to use the gap field for prebunching, the electrodes can be slightly shortened or extended. Thus, the rising edge of the entrance gap induced energy modulation matches a phase of $-90°$ at the center of the first modulated RFQ cell.
- The optimum entrance phase might be experimentally found by a slight variation of the injection energy.
- Calculating the effective phase of the exit gap to determine the energy gain or loss at the high energy end. The exact RFQ exit energy is only derived by including the effect of the exit gap. The phase dependent energy modulation is as large as $\pm 1\%$ typically and should be included in future designs.

The concept proposed here can be applied to any type of 4-Rod RFQ.

6. Outlook

As soon as the Ladder-RFQ as well as the LEBT and source of the p-Linac will have been finalized (2019), both can be installed within the p-Linac building (after 2020). Afterwards, the beam dynamics and beam parameters can be measured and verified. As in the particular case of the 325 MHz p-Linac RFQ the entrance gap effects are modest, there will be more pronounced 4-ROD-RFQ cases for an experimental demonstration of the entrance gap effect. "Easy to measure" are the

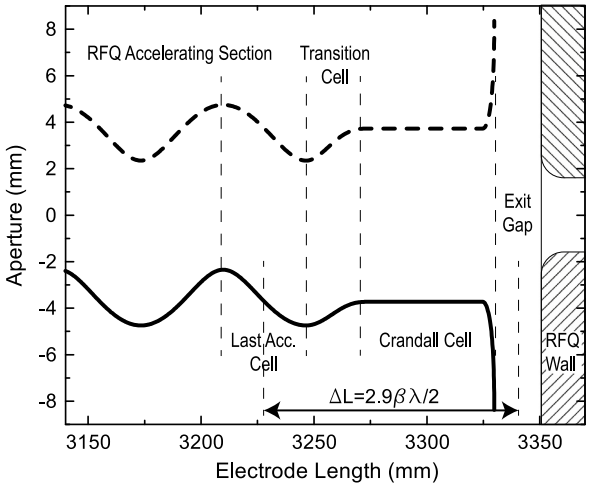

Fig. 11. Detailed view of the electrode modulation at the RFQ exit. Both curves (dashed / "upper" and straight / "lower") represent a pair of opposing electrodes in the horizontal and vertical plane, respectively.

effects on the transverse emittance by the slit-grid emittance measurement technique. Longitudinally, the energy spread can be measured with high precision behind a magnetic spectrometer and the phase width by a Feschenko monitor [13]. Transmission measurements into a specified exit energy windows seem as well reasonable.

References

[1] J.S. Schmidt, B. Koubek, A. Schempp, C.Y. Tan, D.S. Bollinger, K.L. Duel, P.R. Karns, W.A. Pellico, V.E. Scarpine, B.A. Schupbach, S.S. Kurennoy, Investigations of the output energy deviation and other parameters during commissioning of the four-ROD radio frequency quadrupole at the fermi national accelerator laboratory, Phys. Rev. ST Accel. Beams 17 (3) (2014) 030102, http://dx.doi.org/10.1103/physrevstab.17.030102.

[2] K.R. Crandall, RFQ Radial matching sections and fringe fields, in: Proceedings of LINAC84, Seeheim, Germany, 1984, pp. 109–111.

[3] Y. Iwashita, H. Fujisawa, Half end-cell geometry of RFQ, in: Proceedings of LINAC92, Ottawa, Ontario, Canada, 1992, pp. 698–700.

[4] K. Crandall, Ending RFQ vanetips with quadrupole symmetry, in: Proceedings of LINAC94, Tsukuba, Japan, 1994, pp. 227–229.

[5] M. Schuett, U. Ratzinger, M. Syha, Progress of the modulated 325 MHz Ladder RFQ, J. Phys. Conf. Ser. 1067 (5) (2018) 052004, http://dx.doi.org/10.1088/1742-6596/1067/5/052004.

[6] K. Crandall, T. Wangler, PARMTEQ - A beam dynamics code for the RFQ linear accelerator, in: Proceedings of Workshop on Linear Accelerator and Beam Optics Codes, Vol. 177(1), San Diego, CA, USA, 1988, pp. 22–28, http://dx.doi.org/10.1063/1.37798.

[7] M. Syha, M. Schuett, M. Obermayer, U. Ratzinger, Beam dynamics for a high current 3 MeV, 325 MHz ladder-RFQ, in: Proceedings of IPAC17, Copenhagen, Denmark, 2017, pp. 2252–2254, http://dx.doi.org/10.18429/JACoW-IPAC2017-TUPVA075, 8.

[8] M. Syha, U. Ratzinger, M. Schuett, Beam dynamics for the FAIR p-Linac Ladder-RFQ, in: Proceedings of LINAC18, Beijing, China, 2018, pp. 521–523, http://dx.doi.org/10.18429/JACoW-LINAC2018-TUPO083, 29.

[9] M. Schuett, U. Ratzinger, A. Schnase, M. Syha, M. Obermayer, Status of the modulated 3 MeV 325 MHz ladder-RFQ, J. Phys. Conf. Ser. 874 (1) (2017) 012048, http://dx.doi.org/10.1088/1742-6596/874/1/012048.

[10] M. Schuett, U. Ratzinger, M. Syha, First RF measurements of the 325 MHz Ladder-RFQ, in: Proceedings of LINAC18, Beijing, China, 2018, pp. 826–829, http://dx.doi.org/10.18429/JACoW-LINAC2018-THPO060, 29.

[11] C. Kleffner, S. Appel, R. Berezov, J. Fils, P. Forck, M. Kaiser, K. Knie, C. Muehle, S. Puetz, A. Schnase, G. Schreiber, A. Seibel, T. Sieber, V. Srinivasan, J. Trueller, W. Vinzenz, C. Will, A.M. Almomani, H. Haehnel, U. Ratzinger, M. Schuett, M. Syha, Status of the FAIR p-LINAC, in: Proceedings of LINAC18, Beijing, China, 2018, pp. 787–789, http://dx.doi.org/10.18429/JACoW-LINAC2018-THPO046, 29.

[12] U. Ratzinger, The IH-structure and its capability to accelerate high current beams, in: Proceedings of PAC91, San Francisco, USA, 1991, pp. 567–571.

[13] A.V. Feschenko, P. Ostroumov, Bunch shape measuring technique and its application for an ion linac tuning, in: Proceedings of LINAC86, Stanford, CA, USA, 1986, pp. 323–327.